

## Conversion of Electrospun Polyacrylonitrile (PAN) into Carbon Fibres

Marini Sawawi<sup>1,\*</sup>, Cheryl Rinnai Raja<sup>1</sup>, Siti Kudnie Sahari<sup>1</sup>, Sinin Hamdan<sup>1</sup>, Nur Tahirah Razali<sup>1</sup>, and Nicholas Kuan<sup>1</sup>

<sup>1</sup>Faculty of Engineering, Universiti Malaysia Sarawak (UNIMAS), 94300 Kota Samarahan, Sarawak

### ABSTRACT

*Electrospun polyacrylonitrile (PAN) polymer is one of the most often utilised precursors for the synthesis of carbon fibres. In this work, PAN was electrospun prior to stabilisation at 280°C and carbonisation at 1200°C. The carbonisation process has successfully converted the electrospun PAN into carbon fibres with approximately similar diameter produced. The ATR-FTIR spectrum shows the as-received and as-spun PAN have a similar chemical structure showing all the solvent has completely vaporised. The conversion of electrospun PAN into carbon fibres are evident from the ATR-FTIR spectrum and XRD peak. There is no apparent peak in the ATR-FTIR spectrum due to the absorbing nature of black carbon, but the XRD data reveals two diffraction peaks at scattering angles of 25° and 44°, which are identical to those previously described for graphitic structures. The conductivity of the carbonised electrospun PAN was found to be  $14.2 \pm 0.04 \text{ Scm}^{-1}$  which is in agreement with findings from others. This indicates that the carbonisation parameter used in this study is sufficient to synthesize a carbon fibre with a moderate conductivity level which is suitable to be used as electrical conductors or in semiconductor applications.*

**Keywords:** Electrospinning, electrospun PAN, carbonisation, carbon fibres

### 1. INTRODUCTION

Electrospinning is one of the methods to produce fibres in a submicron to nano diameter range effectively. It has been used to produce electrospun PAN which has been popular as a precursor for carbon fibres [1]–[8]. Subsequent carbonisation of the electrospun nanofibrous PAN membranes in an inert environment yields a nanofibrous membrane of pure carbon fibres [9]–[11]. These carbon fibres are of great interest having wide reaching applications including as membrane filters, electronic devices and as composite reinforcement to improve their mechanical properties and impart conductivity where appropriate [12], [13].

Successful conversion of electrospun PAN to carbon fibres varies depending on the stabilisation and carbonisation conditions such as the temperature, the types of inert gas and the heating rate [5]. The low temperature carbonisation stage leads to low degree of carbonisation thus result in lower crystallinity and electrical properties [14]. This is especially true for the electrical properties of the carbon fibres produced where some the conductivity obtained is rather low due to the temperature of the stabilisation and carbonisation stage.

Numerous research has shown the effects of carbonisation process to the chemical structure and the crystal structure of the carbon fibre [5], [12]. However, the whole process of synthesizing the carbon fibres often did not discuss the electrical properties obtained. Thus, in this work, the conversion of the electrospun PAN into carbon fibres is discussed and the electrical property is evaluated.

\* smarini@unimas.my

## 2. EXPERIMENTAL METHODS

### 2.1 Materials

The materials used in this work are polyacrylonitrile (PAN) with a molecular weight of 120,000 (Sigma Aldrich), dimethylformamide (DMF) (Merck Pty Ltd) and deionised water (Direct-Q3 water purification system, Millipore).

### 2.2 Electrospinning

For the electrospinning process, custom-built electrospinner powered by a high voltage source from Gamma High Voltage Research (USA) was used, while the syringe pump came from Razel Scientific Instruments, Inc. (USA). Polymer solution preparation was done by dissolving the as received PAN powder at room temperature overnight in DMF at 10 wt/v% using a magnetic stirrer prior to electrospinning. The polymer solution was then injected into a 10 mL syringe and electrospun at 20 kV, 6 cm working distance, and 18G needle size. The electrospun membrane was collected on a rotating mandrel that had a 0.32 m/s speed. Importantly, this relatively low rotation velocity still results in randomly aligned electrospun membranes, with the method being employed to increase the collection area and uniformity of the membrane.

### 2.3 Carbonisation

Carbonisation of PAN electrospun fibres involved two stages, with the first being the stabilisation and carbonisation stage using a tube furnace (KMT-GSL-1600X). Stabilisation involved heat treatment of electrospun PAN up to 280 °C in air (oxygen) for 1 hr to allow oxidation to take place. The second stage was the carbonisation that was performed at 1200 °C in high purity Argon for 1 hr. The temperature and holding time were selected based on the common temperature for stabilisation which ranges from 200 °C to 300 °C while the carbonisation was usually conducted at the temperature of 1000 °C to 1500 °C with the holding time of 1 hr for each step to ensure complete chemical reaction takes place [5]. Briefly, the electrospun PAN membranes were cut to size and placed layer-by-layer in an alumina crucible. The tube furnace's crucible was centrally located to provide better heat distribution. During the initial stage of carbonisation, the tube was kept open to ensure complete oxidation. After stabilisation, the furnace was evacuated followed by purging with Argon gas for 3 times to ensure a completely inert atmosphere. The temperature was then raised to 1200 °C at 2 °C/min and maintained for one hour in order to facilitate carbonisation. A minimal amount of Argon gas was maintained using the bubbler throughout the carbonisation and cooling process.

### 2.4 Characterisation

Field Emission Scanning Electron Microscope (JEOL 7001FEG SEM) at 15kV was used to characterise the morphology of as-spun fibres and short fibres. After air drying in a fume hood for a night, samples were sputter coated with platinum (to a thickness of around 1 nm) using Cressington 208HR, UK before being imaged.

Further characterisation was performed by Attenuated Total Reflectance Fourier Transform Infrared spectroscopy (ATR-FTIR) utilising a Thermo Scientific Nicolet 6700 scanning from 4500 to 400  $\text{cm}^{-1}$  and 4  $\text{cm}^{-1}$ . Electrospun and short fibre samples were placed firmly onto the ATR crystal before being measured.

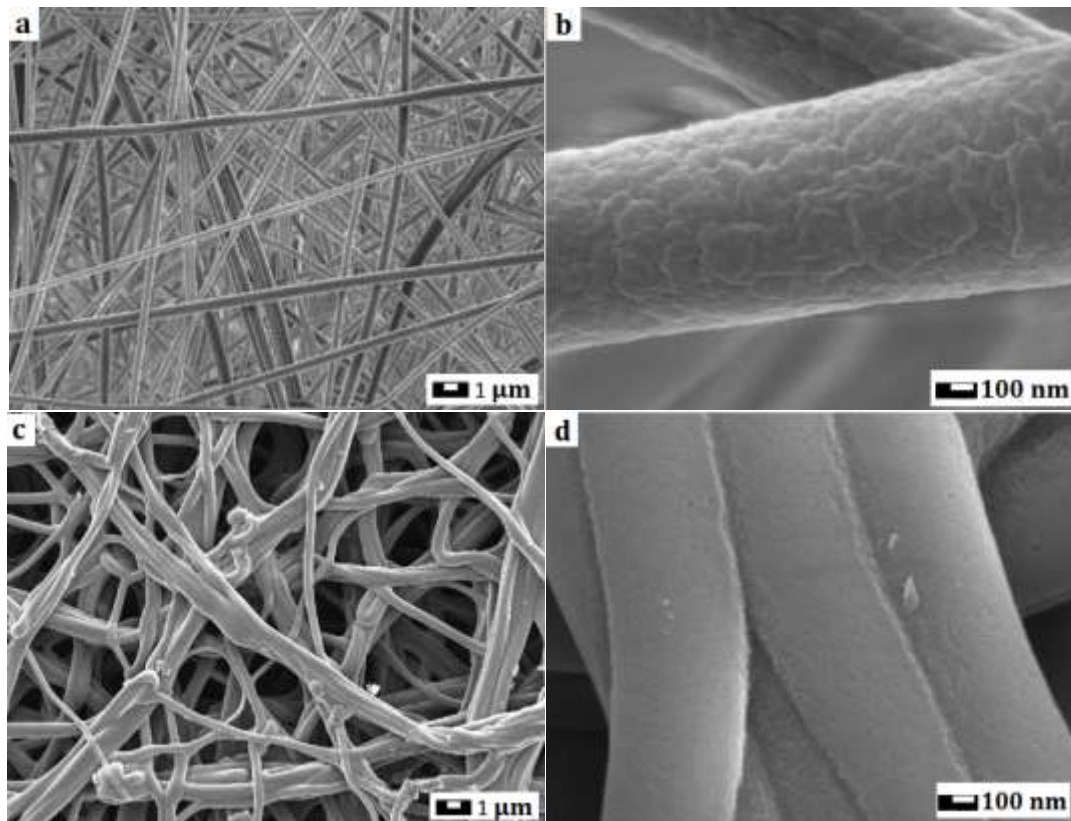
Crystallinity, phase confirmation, and average crystal size are all assessed using X-ray diffraction (XRD). The X-ray diffraction (XRD) spectra were acquired using a Phillips 1140 diffractometer with a copper target ( $\text{Cu K}\alpha$ ) at a scan rate of 2°/min and with discrete 0.02° steps at a wavelength of  $\lambda = 0.1541 \text{ nm}$ .

The electrical resistivity was measured with a conventional 4-point probe (RM3-AR from Jandel Engineering, UK) that has four tungsten metal tips spaced equally apart (0.5 mm). For carbonised electrospun PAN measurement, the electrospun membrane were compacted prior carbonisation so that they become flat. The instrument was calibrated and test with the standard material to ensure the reliability and accuracy of the measurement. The averages of measurements taken from at least 5 distinct locations on each specimen were calculated.

### 3. RESULTS AND DISCUSSION

#### 3.1 Scanning Electron Microscopy (SEM)

Physically, the originally white electrospun membrane became black, in addition to showing considerable shrinkage of the webs when they are carbonised. The color change was due to the structural changes where nitrile group ( $C \equiv N$ ) converts into imine double bonds ( $C = N$ ), forming a ladder structure[15]. Observation from SEM can be seen in Figure 1.



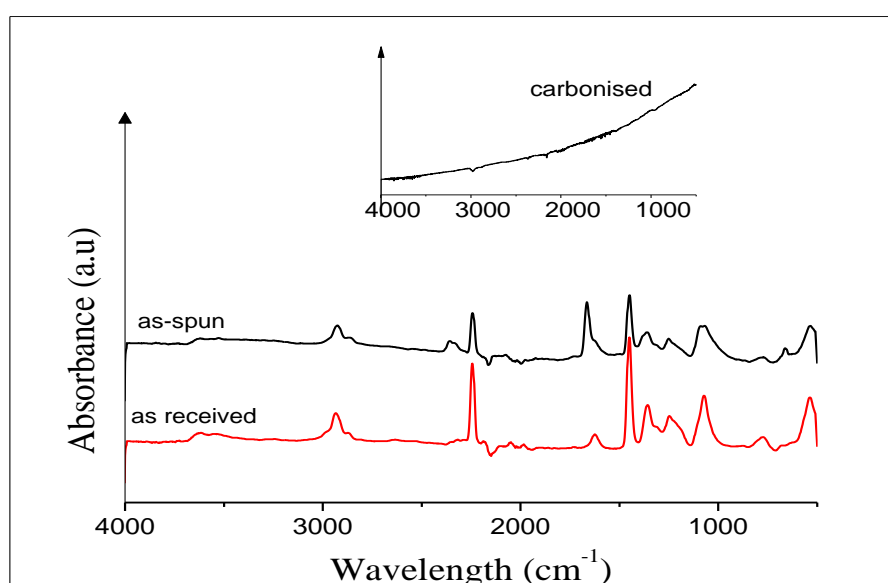
**Figure 1.** SEM images of a,b) As-spun electrospun PAN, c,d) carbonised electrospun PAN.

Figure 1 shows that post carbonisation of the as-spun membranes, the surface topography of the nanofibers had a much smoother morphology (Figure 1d), with the initial nanoroughness being significantly reduced (Figure 1b). In addition, it appeared as if fibre relaxation had occurred post carbonisation (Figure 1c) evident by them displaying a 'wavy' morphology compared to the initial long, relatively straight as-spun fibres (Figure 1a) [16]. According to earlier research, the relaxation is probably caused by the uneven inner stress that develops around the outer surface as the dehydrogenation reaction progresses [17], where volatile molecules like water are expelled. Long continuous fibres that are in close proximity to neighbouring fibres experienced some fusion as can be seen in Figure 1c.

The carbonisation leads to a small reduction in diameter which is from  $620 \pm 123$  nm to  $580 \pm 178$  nm. The production of carbon basal planes caused the arrangement and compactness of structures along the fibre axis, which in turn led to an increase in density [17], [18]. As a result, the diameter of the carbonised fibres was reduced.

### 3.2 ATR-FTIR Spectra

The ATR-FTIR spectrum (Figure 2) revealed that the methylene group stretching vibration appeared at  $2923\text{ cm}^{-1}$  and  $2867\text{ cm}^{-1}$  in the as-received PAN powder and as-spun PAN membrane. The strong peak at  $2240\text{ cm}^{-1}$  was the nitrile group's characteristic vibration absorption ( $-\text{CN}-$ ). Carbon-carbon double bond stretching vibrations were detected at  $1660\text{ cm}^{-1}$  and  $1630\text{ cm}^{-1}$ . The bending vibrations of the methylene and methane groups were assigned to the peaks at  $1452\text{ cm}^{-1}$  and  $1361\text{ cm}^{-1}$ , respectively. The vibration of the methane group caused the  $1253\text{ cm}^{-1}$  peak. When the spectra were compared, it was discovered that there was an additional weak band at  $2356\text{ cm}^{-1}$  and  $2321\text{ cm}^{-1}$  for the as-spun membrane, which was caused by  $\text{CO}_2$  and can be ignored.



**Figure 2.** ATR-FTIR spectra for as received PAN, as-spun electrospun membrane and carbonised electrospun PAN.

The ATR-FTIR for carbonised samples showed that the electrospun PAN has been fully converted into carbon fibres, where no infra-red peaks were observed due to the absorbing nature of black carbon samples [19], [20].

### 3.3 X-Ray diffraction (XRD)

Figure 3 shows two diffraction peaks at  $2\theta$  scattering angles of  $25^\circ$  and  $44^\circ$ , which are close to those previously reported for the graphitic structures [20]. From XRD data, the size of crystallite  $L_c$  and  $L_a$ , along  $c$ - and  $a$ -directions can be calculated from the Bragg and Scherrer equation as follows [21]:

$$L_c = \frac{0.9\lambda}{\beta \cos \theta} \quad (1)$$

$$L_a = \frac{1.84\lambda}{\beta \cos \theta} \quad (2)$$

where  $L_c$  and  $L_a$  is the crystallite size attributed to the (002) and (10) crystallographic plane of graphite crystallites which is shown by the diffraction peak around  $2\theta$  angle of  $24^\circ$  and  $44^\circ$  respectively.  $\lambda$  is the wavelength of Cu  $K\alpha$  X-ray,  $\beta$  is the full width at half the maximum intensity (FWHM) at (002) and (10) peak.

Using this XRD data, the size of crystallite  $L_c$  and  $L_a$ , were calculated with  $\lambda = 0.154$  nm,  $\beta = 0.08$  rad and  $\theta = 0.21$  rad ( $2\theta = 24.5^\circ$ ), the crystallite size at (002) plane,  $L_c$  is 1.77 nm and the crystallite size at (10) plane,  $L_a$  is 5.10 nm with  $\beta = 0.06$  rad and  $\theta = 0.39$  rad ( $2\theta = 44.2^\circ$ ).

Compared with literature, the  $L_c$  value obtained in this study was within the range obtained by others where Zhou et al [21] obtained 0.882 nm and 1.17 nm (carbonisation temperature of 1000 °C and 1400 °C), whilst Ji et al [18] produced an average of 1.76 nm crystallite size (carbonisation temperature of 1280 °C – 1400 °C). Kim et al [16] found a higher  $L_c$  size of 2.15 nm (carbonisation temperature 1000 °C in Argon) and  $L_a$  size is 3.36 nm. The difference in the crystallite size for this study and that reported in the literature was likely due to the difference in carbonisation parameters such as temperature (larger crystallite size with increasing temperature), purge gas and stabilisation steps used and the initial fibre diameter.

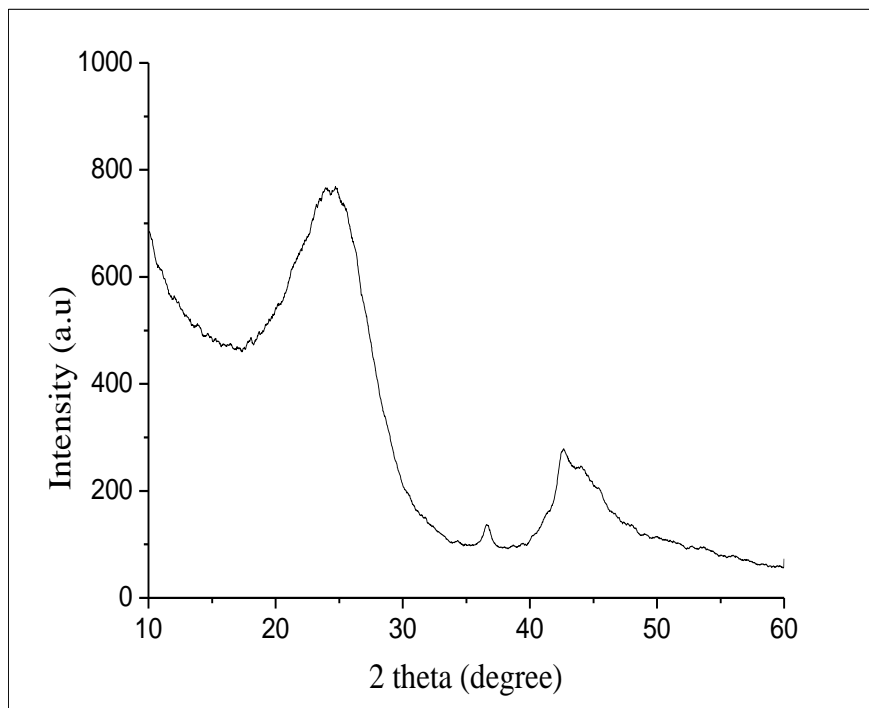


**Figure 3.** XRD curves of carbonised electrospun PAN.

### 3.4 Electrical Resistivity Measurements

The bulk resistivity calculated for the carbonised electrospun PAN is  $0.07 \pm 0.02 \Omega \cdot \text{cm}$ . The conductivity of the sample was the reciprocal of bulk resistivity, and can thus determined to be  $14.2 \pm 0.04 \text{ Scm}^{-1}$ . This is broadly similar to the conductivity of the carbon fibre mat obtained by Kim et al and Liu et al, which is  $1.9 \text{ Scm}^{-1}$  [16] and  $55.41 \text{ Scm}^{-1}$  [22] for the carbonisation temperatures of 1000 °C and 2000 °C, respectively. This shows the carbonisation process has successfully produced a carbon fibre having a moderate conductivity level using the 1200°C carbonisation temperature.

#### 4. CONCLUSION

This research has demonstrated the the synthesis of carbon fibres using electrospun PAN as the precursor. The carbon fibres has been confirmed using ATR-FTIR spectra where no peak observed and the XRD measurement obtained diffraction peaks at  $2\theta$  scattering angles of  $25^\circ$  and  $44^\circ$ , which are close to those previously reported for the graphitic structures. The stabilisation stage at  $280^\circ\text{C}$  and carbonisation temperature at  $1200^\circ\text{C}$  has successfully converted the electrospun fibres into carbon fibres that is having the electrical conductivity of  $14.2 \pm 0.04 \text{ Scm}^{-1}$ .

#### ACKNOWLEDGEMENT

Fundamental Research Grant Scheme (FRGS) (FRGS/1/2020/TK0/UNIMAS/02/12) from the Ministry of Higher Education, Malaysia and Universiti Malaysia Sarawak (F02/FRGS/1999/2020) are acknowledged for funding this study.

#### REFERENCES

- [1] S.K. Nataraj, K.S. Yang, and T.M. Aminabhavi, Polyacrylonitrile-based nanofibers—A state-of-the-art review', *Progress in Polymer Science* 37, (2012) 487–513.
- [2] N. Yusof and A.F. Ismail, Post spinning and pyrolysis processes of polyacrylonitrile (PAN)-based carbon fiber and activated carbon fiber: A review, *Journal of Analytical and Applied Pyrolysis* 93 (2012) 1–13.
- [3] K. Şahin et al., High strength micron size carbon fibers from polyacrylonitrile–carbon nanotube precursors, *Carbon* 77, (2014) 442–453.
- [4] N. Hameed et al., Structural transformation of polyacrylonitrile fibers during stabilization and low temperature carbonization, *Polymer Degradation and Stability* 128, (2016) 39–45.
- [5] R. Shokrani Havigh and H. Mahmoudi Chenari, A comprehensive study on the effect of carbonization temperature on the physical and chemical properties of carbon fibers, *Scientific Reports* 12, (2022) 1–14.
- [6] O. Zaca-Moran, J. F. Sánchez-Ramírez, J.L. Herrera-Pérez, and J. Díaz-Reyes, Electrospun polyacrylonitrile nanofibers as graphene oxide quantum dot precursors with improved photoluminescent properties, *Materials Science in Semiconductor Processing* 127, (2021) 105729.
- [7] S. Dong et al., Excellent microwave absorption of lightweight PAN-based carbon nanofibers prepared by electrospinning, *Colloids and Surfaces A: Physicochemical and Engineering Aspects* 651, (2022) 129670.
- [8] J.L. Storck et al., Comparative Study of Metal Substrates for Improved Carbonization of Electrospun PAN Nanofibers, *Polymers* 14, (2022) 721.
- [9] E.A. Morris et al., High performance carbon fibers from very high molecular weight polyacrylonitrile precursors, *Carbon* 101, (2016) 245–252.
- [10] Q.S. Ma, A.J. Gao, Y.J. Tong, and Z.G. Zhang, The densification mechanism of polyacrylonitrile carbon fibers during carbonization, *New Carbon Materials* 31, (2016) 550–554.
- [11] N.V. Salim, S. Blight, C. Creighton, S. Nunna, S. Atkiss, and J. M. Razal, The Role of Tension and Temperature for Efficient Carbonization of Polyacrylonitrile Fibers: Toward Low Cost Carbon Fibers, *Industrial & Engineering Chemistry Research* 57, (2018) 4268–4276.
- [12] R. Schierholz et al., The carbonization of polyacrylonitrile-derived electrospun carbon nanofibers studied by: In situ transmission electron microscopy, *RSC Advances* 9, (2019) 6267–6277.
- [13] J.P. Lee, S. Choi, S. Cho, W.J. Song, and S. Park, Fabrication of carbon nanofibers decorated with various kinds of metal oxides for battery applications, *Energies* 14, (2021) 1353.

- [14] J.L. Storck et al., Stabilization and carbonization of PAN nanofiber mats electrospun on metal substrates, *Journal of Carbon Research* 7, (2021) 12.
- [15] M.S.A. Rahaman, A.F. Ismail, and A. Mustafa, A review of heat treatment on polyacrylonitrile fiber, *Polymer Degradation and Stability* 92, (2007) 1421–1432.
- [16] C. Kim et al., Raman spectroscopic evaluation of polyacrylonitrile-based carbon nanofibers prepared by electrospinning, *Journal of Raman Spectroscopy* 35, (2004) 928–933.
- [17] J. Zhu, S. Wei, D. Rutman, N. Haldolaarachchige, D.P. Young, and Z. Guo, Magnetic polyacrylonitrile-Fe@FeO nanocomposite fibers - Electrospinning, stabilization and carbonization, *Polymer* 52, (2011) 2947–2955.
- [18] M. Ji, C. Wang, Y. Bai, M. Yu, and Y. Wang, Structural Evolution of Polyacrylonitrile Precursor Fibers during Preoxidation and Carbonization, *Polymer Bulletin* 59, (2007) 527–536.
- [19] Z. Wangxi, L. Jie, and W. Gang, Evolution of structure and properties of PAN precursors during their conversion to carbon fibers, *Carbon* 41, (2003) 2805–2812.
- [20] J. Sutasinpromprae, S. Jitjaicham, M. Nithitanakul, C. Meechaisue, and P. Supaphol, Preparation and characterization of ultrafine electrospun polyacrylonitrile fibers and their subsequent pyrolysis to carbon fibers, *Polymer International* 55, (2006) 825–833.
- [21] Z. Zhou et al., Development of carbon nanofibers from aligned electrospun polyacrylonitrile nanofiber bundles and characterization of their microstructural, electrical, and mechanical properties, *Polymer* 50, (2009) 2999–3006.
- [22] C.-K. Liu, K. Lai, W. Liu, M. Yao, and R.-J. Sun, Preparation of carbon nanofibres through electrospinning and thermal treatment, *Polymer International* 58, (2009) 1341–1349.

